

# An ion-exchanged $\text{Tm}^{3+}$ :glass channel waveguide laser

Amol Choudhary,\* Pradeesh Kannan, Jacob I. Mackenzie, Xian Feng, and David P. Shepherd

*Optoelectronics Research Centre, University of Southampton, Highfield, Southampton, UK, SO17 1BJ*

*\*Corresponding author*

**Continuous wave laser action around 1.9  $\mu\text{m}$  has been demonstrated in a  $\text{Tm}^{3+}$  - doped germanate glass channel waveguide laser fabricated by ion-exchange. Laser action was observed with an absorbed power threshold of only 44mW and a slope efficiency of up to 6.8 % was achieved. Propagation loss at the lasing wavelength was measured and found to be 0.3 dB/cm. We believe this to be the first ion-exchanged  $\text{Tm}^{3+}$ -doped-glass waveguide laser.**

Recent development of solid-state lasers operating in the eye-safe region near 2 micron has been motivated by potential applications in spectroscopy [1], medicine [2] and LIDAR [3]. The  $^3\text{F}_4 \rightarrow ^3\text{H}_6$  transition of the Thulium ( $\text{Tm}^{3+}$ ) ion is widely used for making lasers operating near 2  $\mu\text{m}$ .  $\text{Tm}^{3+}$ -doped gain media benefit from a broad absorption band near 800 nm that can be pumped by commercially available laser diodes, a broad emission bandwidth which can be exploited for the generation of ultrafast lasers [4] and the possibility of having a quantum efficiency of 2 due to cross relaxation between the  $^3\text{H}_4$  and  $^3\text{H}_6$  levels.

$\text{Tm}^{3+}$  lasers operating at 2  $\mu\text{m}$  suffer from reabsorption losses, resulting in higher threshold powers when compared to pure 4-level laser systems. By employing a waveguide geometry, the threshold power can be reduced because of the tight confinement of the pump and laser modes. Guided-wave devices offer additional advantages of compactness and integration and good thermal management for high power operation [5].  $\text{Tm}^{3+}$ -doped waveguide laser action has been demonstrated in several crystal hosts [5-12]. However, laser operation in  $\text{Tm}^{3+}$ -doped glass waveguide hosts has been limited to ion-implanted lead germanate [13] and femtosecond written fluorogermanate [14] and ZBLAN [15] glass.

Here we demonstrate the first, to the best of our knowledge ion-exchanged  $\text{Tm}^{3+}$ :glass waveguide laser operation. We employ a novel combination of ion-beam milling and ion-exchange to fabricate low-loss waveguides which exhibit lasing with an absorbed threshold power as low as 44 mW.

Glass laser hosts are relatively cheap and easy to fabricate and ion-exchange is a widely used technique of low-loss waveguide fabrication in glasses [16]. We have recently demonstrated multi-GHz repetition rate, femtosecond operation of an ion-exchanged Yb:glass waveguide laser at 1  $\mu\text{m}$  [17] and extension of this work to 2  $\mu\text{m}$  would open up opportunities such as pumping of mid-infrared frequency combs [18]. However, to date there have been very limited reports [19, 20] of ion-exchanged  $\text{Tm}^{3+}$  glass waveguides and a focus has been on amplification near 1.5  $\mu\text{m}$  [20].

$\text{Tm}^{3+}$ :germanate glass with a composition of 65.5  $\text{GeO}_2$  - 12  $\text{Al}_2\text{O}_3$  - 4.5  $\text{BaO}$  - 18  $\text{Na}_2\text{O}$  (mol %) and doped with 1

mol %  $\text{Tm}_2\text{O}_3$  was fabricated by a standard melting and quenching technique. Annealed glasses were then sliced to dimensions of 20 mm x 20 mm x 2 mm and were surface polished for channel waveguide fabrication. A  $35 \pm 5$  nm aluminium (Al) film was deposited on the polished glass by an electron-beam evaporation system following which, the polished glasses were photo-lithographically patterned to define a mask with channel openings with widths between 1  $\mu\text{m}$  and 10  $\mu\text{m}$  in steps of 0.2  $\mu\text{m}$ . In the first instance, following standard processing steps, a chemical etchant (Al etchant by OM group) was used to etch the Al film [17], however it was found that the glass also reacted with the etchant resulting in a very rough surface. To overcome this,  $\text{Ar}^+$  ion-beam milling was used to etch the Al film and to define the metal mask. The etching parameters were: current = 100 mA, voltage = 500 V and time = 150 seconds. The photoresist was removed by using solvents and the glass was then ion-exchanged with a melt composition of 43 mol%  $\text{KNO}_3$  - 55 mol%  $\text{NaNO}_3$  - 2 mol%  $\text{AgNO}_3$  at 300°C for 20 min. After ion-exchange, the Al mask was removed by  $\text{Ar}^+$  ion beam milling and the end facets of the glass were polished to a length of 11.5 mm. Since ion-beam milling is a physical process with low selectivity; the glass was also etched by 50 nm as seen from figure 1.

The refractive index profile was measured in a planar ion-exchanged waveguide by m-line measurements using the prism-coupling method and the diffusion depth was found to be 4.6  $\mu\text{m}$  and the index change ( $\Delta n$ ) was measured to be 0.06 at 1553 nm. The index contrast can also be seen in figure 1. From m-lines measurements it was found that the waveguide supports 5 modes at 633 nm, 2 modes at 1553 nm and 1 mode at 1900 nm.

The absorption spectrum of the bulk glass was measured by a Cary 500 spectrophotometer (Varian Ltd, Oxford, UK) and a peak of absorption ( $\alpha$ ) of  $2.3 \text{ cm}^{-1}$  at 790 nm was measured as seen from figure 2. To the measured absorption spectra, we applied a McCumber analysis [21, 22] to calculate the emission cross sections as shown in the inset of figure 2. It can be seen that the peak of the emission cross section is at 1865 nm with a value of  $2.3 \times 10^{-21} \text{ cm}^2$ .

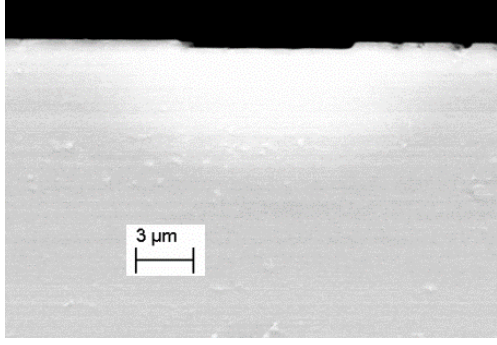


Fig. 1. SEM image (using a backscatter detector) of the cross-section of the ion-exchanged Tm:germanate waveguide.

The Tm<sup>3+</sup>:germanate glass waveguide was mounted on a Peltier-cooled copper mount kept at a constant temperature of 15°C. A titanium sapphire laser tuned to the peak of absorption at 790 nm and delivering up to 500 mW was used as the pump source. A variable neutral density filter was used to control the pump power incident on the waveguide and a half wave plate was used to control the polarization. An 11-mm aspheric lens was used to couple the pump beam into the waveguides. A chopper was installed after the half wave plate and the output from the waveguide was focused on an InGaAs detector to study the fluorescence lifetime of the Tm<sup>3+</sup>:germanate glass at 2 μm, resulting in a value of 0.8 ms.

The pump mode was captured by imaging the output of the waveguide on a CCD camera and is shown in figure 3 a. The 1/e<sup>2</sup> beam radii were measured to be 6.2 μm (x) and 3.2 μm (y) in the horizontal and vertical directions respectively. The mode was simulated by using the index profile (inset of figure 1) in a commercial software (RSoft). The simulated mode sizes were found to be 5.1 μm (x) and 2.1 μm (y) in the horizontal and vertical directions respectively. The discrepancy between these values may be due to the 50 nm etch in the waveguide (as seen from figure 1), which is not included in the model.

A high reflectivity (HR) thin (thickness = 175 μm) dielectric mirror (with a reflectivity > 99.8% at the lasing wavelength and 32% at the pump wavelength) was butted onto the input facet of the waveguide using a fluorinated liquid (Sigma Aldrich, FC-70) for adhesion. An HR/HR laser cavity was formed by butting another HR mirror on the end facet. Laser action was observed for an absorbed power of 44 mW and the lasing wavelength ( $\lambda_{\text{lasing}}$ ) was measured by a Yokogawa AQ6375 optical spectrum analyzer (OSA) to be centered at 1885 nm. The output power was measured by a thermal detector with an RG-1000 filter to separate the pump and was found to be less than 0.5 mW for the maximum pump power. The angular frequency of the relaxation oscillations ( $\omega$ ) was measured at different pump powers using an InGaAs detector. The cavity loss was then estimated [23] by plotting  $\omega^2$  vs.  $r$  (which is  $P/P_{\text{th}} - 1$ , where  $P$  is the pump power and  $P_{\text{th}}$  is the threshold power) as shown in figure 3 b. From the value of cavity loss, the upper limit for the propagation loss was estimated to be 0.3 dB/cm.

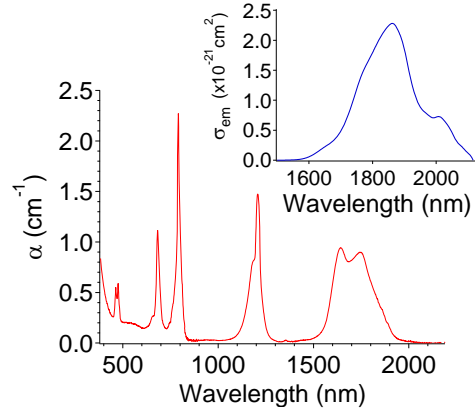


Fig. 2. The absorption spectrum for the Tm:germanate glass measured using a photospectrometer. Inset shows the emission cross section ( $\sigma_{\text{em}}$ ) using McCumber analysis.

Bulk mirrors (thickness = 6 mm) with a transmission of 6% and 10% at the lasing wavelength were put on kinematic mounts and aligned with the waveguide by controlling the tip, tilt and distance between the mirror and the waveguide to achieve efficient laser action. For the 6% and 10% output coupler (OC), lasing was observed at an absorbed threshold power of 69 mW and 78 mW with slope efficiencies 4.3% and 6.8%, respectively. The output power vs. absorbed power for both the output couplers is shown in figure 4. The laser spectra were centered at 1884 nm and 1881 nm for the 6% and 10% OC. The Lasing spectrum obtained with the 10% OC is shown in the inset of figure 4. Relaxation oscillations were measured for both the OCs and the total cavity loss was found to be 1.5 dB more than the HR/HR case. We attribute this additional loss to the misalignment between the bulk mirrors and the waveguides.

The internal quantum efficiency ( $\eta_q$ ) has been estimated to be  $\sim 1.15$  by fitting equation 1 to the measured slope efficiency ( $\eta$ ), using the known pump frequency ( $\nu_p$ ), laser frequency ( $\nu_l$ ), the output transmission ( $T$ ), losses ( $L$ ) measured from the relaxation oscillations and estimating the overlap efficiency ( $\eta_{ol}$ ) from the quasi-3-level analysis of Risk [24].

$$\eta = \frac{\nu_p}{\nu_l} \eta_q \eta_{ol} \frac{T}{T + L} \quad (1)$$

This value indicates that we are benefiting from some

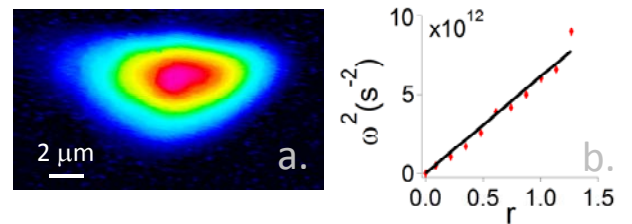


Fig. 3. (a) Pump mode profile measured by a CCD camera and (b)  $\omega^2$  vs.  $r$  for the HR/HR cavity. Red- experimental data, Black – linear fit.

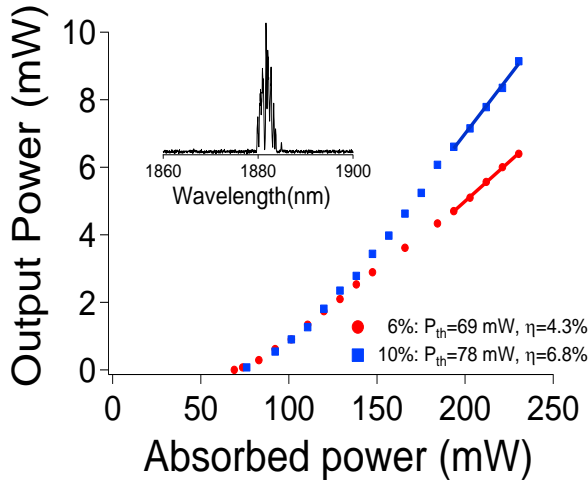


Fig. 4. Output power vs. absorbed power for a  $\text{Tm}^{3+}$ :germanate glass waveguide laser using a 6% and 10% output coupler. The inset shows the laser spectrum centred at 1881 nm, obtained with a 10% output coupler.

cross-relaxation helping to populate the upper laser level but that higher  $\text{Tm}^{3+}$  doping may be more favorable. Using this value of  $\eta_q$ , the threshold values have been calculated [13] for the different cavity configurations and are presented in table 1. It can be seen that there is a good agreement between measured values and theoretical values of the threshold power.

**Table 1. Summary of results for  $\text{Tm}$ :germanate waveguide laser**

Output Coupler	$P_{th}$ Measured (mW)	$P_{th}$ Theory (mW)	Slope Efficiency (%)	$\lambda_{lasing}$ (nm)
HR	44	37	-	1885
6%	69	64	4.3	1884
10%	78	67	6.8	1881

In summary, we have demonstrated the first ion-exchanged  $\text{Tm}^{3+}$  glass waveguide laser. Laser action was observed between 1881 nm and 1885 nm for different OCs. Threshold power as low as 44 mW was observed for an HR/HR cavity and a slope efficiency of 6.8% was observed for a cavity formed by a thin dielectric HR mirror a bulk OC. The laser performance can be improved by (1) higher doping of  $\text{Tm}^{3+}$  in the glass matrix to increase the internal quantum efficiency and (2) using thin dielectric mirrors or direct coating rather than bulk mirrors to reduce the cavity loss. Efficient ion-exchanged  $\text{Tm}$ : glass waveguides promise a cheap and durable platform to achieve fully integrated on-chip modelocked sources around 2  $\mu\text{m}$ .

This work was supported by the UK Engineering and Physical Sciences Research Council (EPSRC) under projects EP/H035745/1 and EP/J008052/1. We also acknowledge Neil Sessions and Dave Sager for their technical support in the integrated photonics cleanroom. Useful discussions with Dr. Senthil Ganapathy are also acknowledged.

## References

1. B. M. Walsh, *Laser Phys.* **19**, 855-866 (2009).
2. D. Theisen, V. Ott, H. W. Bernd, V. Danicke, R. Keller, and R. Brinkmann, *Proc. SPIE* **5142**, 96 (2003).
3. S. W. Henderson, P. J. M. Suni, C. P. Hale, S. M. Hannon, J. R. Magee, D. L. Bruns, and E. H. Yuen, *IEEE Trans. Geosci. Remote Sens.* **31**, 4-15 (1993).
4. A. A. Lagatsky, S. Calvez, M. D. Dawson, J. A. Gupta, V. E. Kisel, N. V. Kuleshov, C. T. A. Brown, M. D. Dawson, and W. Sibbett, *Opt. Express* **19**, 9995-10000 (2011).
5. J. I. Mackenzie, S. C. Mitchell, R. J. Beach, H. E. Meissner, D. P. Shepherd, *Electron. Lett.* **37**, 898-899, (2001).
6. A. Rameix, C. Borel, B. Chambaz, B. Ferrand, D.P. Shepherd, T. J. Warburton, D. C. Hanna, A. C. Tropper, *Opt. Comm.* **142**, 239-243 (1997).
7. W. Bolanos, F. Starecki, A. Benayad, G. Brasse, V. Ménard, J. Doualan, A. Braud, R. Moncorgé, and P. Camy, *Opt. Lett.* **37**, 4032-4034 (2012).
8. S. Rivier, X. Mateos, V. Petrov, U. Griebner, Y. Romanyuk, C. Borca, F. Gardillou, and M. Pollnau, *Opt. Express* **15**, 5885-5892 (2007).
9. J. P. de Sandro, J. K. Jones, D. P. Shepherd, M. Hempstead, J. Wang, A. C. Tropper, *IEEE Photon. Technol. Lett.* **8**, 209-211 (1996).
10. K. van Dalen, S. Aravazhi, C. Grivas, S. García-Blanco, and M. Pollnau, *Opt. Lett.* **37**, 887-889 (2012).
11. E. Cantelar, J. A. Sanz-Garcia, G. Lifante, F. Cusso, and P. L. Pernas, *Appl. Phys. Lett.* **86**, 161119 (2005).
12. W. Bolaños, J. Carvajal, X. Mateos, E. Cantelar, G. Lifante, U. Griebner, V. Petrov, V. Panyutin, G. Murugan, J. Wilkinson, M. Aguiló, and F. Díaz, *Opt. Express* **19**, 1449-1454 (2011).
13. D. Shepherd, D. Brinck, J. Wang, A. Tropper, D. Hanna, G. Kakarantzias, and P. Townsend, *Opt. Lett.* **19**, 954-956 (1994).
14. F. Fusari, R. Thomson, G. Jose, F. Bain, A. Lagatsky, N. Psaila, A. Kar, A. Jha, W. Sibbett, and C. Brown, *Opt. Lett.* **36**, 1566-1568 (2011).
15. D. Lancaster, S. Gross, H. Ebendorff-Heidepriem, K. Kuan, T. Monro, M. Ams, A. Fuerbach, and M. Withford, *Opt. Lett.* **36**, 1587-1589 (2011).
16. R. V. Ramaswamy, R. Srivastava, *J. Lightw. Technol.* **6**, 984-1000 (1988).
17. A. Choudhary, A. A. Lagatsky, K. Pradeesh, W. Sibbet, C. T. A. Brown, D. P. Shepherd, *Opt. Lett.* **37**, 4416-4418 (2012).
18. N. Leindecker, A. Marandi, R. Byer, K. Vodopyanov, J. Jiang, I. Hartl, M. Fermann, and P. Schunemann, *Opt. Express* **20**, 7046-7053 (2012).
19. T. Luo, S. Jiang, Y. Hu, G. N. Conti, S. Honkanen, S. B. Mendes, N. Peyghambarian, *Quantum Electronics and Laser Science Conference, 1999. QELS '99* **266** (1999).
20. D. L. Yang, E. Y. B. Pun, and H. Lin, *Appl. Phys. Lett.* **95**, 151106 (2009).
21. D. E. McCumber, *Phys. Rev.* **136**, A954-A957 (1964).
22. L. Zhang, J. Zhang, C. Yu, and L. Hu, *J. Appl. Phys.* **108**, 103117 (2010).
23. J.R. Salcedo, J.M. Sousa and V.V. Kuzmin, *Appl. Phys. B*, **62**, 83-85 (1996).
24. W. Risk, *J. Opt. Soc. Am. B* **5**, 1412-1423 (1988).

## References (with titles)

1. B. M. Walsh, "Review of Tm and Ho materials: spectroscopy and lasers," *Laser Phys.* **19**, 855-866 (2009).
2. D. Theisen, V. Ott, H. W. Bernd, V. Danicke, R. Keller, and R. Brinkmann, "Cw high-power IR-laser at 2  $\mu\text{m}$  for minimally invasive surgery," *Proc. SPIE* **5142**, 96 (2003).
3. S. W. Henderson, P. J. M. Suni, C. P. Hale, S. M. Hannon, J. R. Magee, D. L. Bruns, and E. H. Yuen, "Coherent laser-radar at 2  $\mu\text{m}$  using solid-state lasers," *IEEE Trans. Geosci. Remote Sens.* **31**, 4-15 (1993).
4. A.A. Lagatsky, S. Calvez, M.D. Dawson, J.A. Gupta, V.E. Kisel, N.V. Kuleshov, C.T.A. Brown, M.D. Dawson, and W. Sibbett, "Broadly tunable femtosecond mode-locking in a Tm:KYW laser near 2  $\mu\text{m}$ ," *Opt. Express* **19**, 9995-10000 (2011).
5. J.I. Mackenzie, S.C. Mitchell, R.J. Beach, H.E. Meissner, D.P. Shepherd, "15 W diode-side-pumped Tm:YAG waveguide laser at 2  $\mu\text{m}$ ," *Electron. Lett.* **37**, 898-899, (2001).
6. A. Rameix, C. Borel, B. Chambaz, B. Ferrand, D.P. Shepherd, T.J. Warburton, D.C. Hanna, A.C. Tropper, "An efficient, diode-pumped, 2  $\mu\text{m}$  Tm:YAG waveguide laser," *Opt. Comm.* **142**, 239-243 (1997).
7. W. Bolanos, F. Starecki, A. Benayad, G. Brasse, V. Ménard, J. Doualan, A. Braud, R. Moncorgé, and P. Camy, "Tm:LiYF<sub>4</sub> planar waveguide laser at 1.9  $\mu\text{m}$ ," *Opt. Lett.* **37**, 4032-4034 (2012).
8. S. Rivier, X. Mateos, V. Petrov, U. Griebner, Y. Romanyuk, C. Borca, F. Gardillou, and M. Pollnau, "Tm:KY(WO<sub>4</sub>)<sub>2</sub> waveguide laser," *Opt. Express* **15**, 5885-5892 (2007).
9. J.P. de Sandro, J.K. Jones, D.P. Shepherd, M. Hempstead, J. Wang, A.C. Tropper, "Non-photorefractive CW Tm-indiffused Ti:LiNbO<sub>3</sub> waveguide laser operating at room temperature," *IEEE Photon. Technol. Lett.* **8**, 209-211 (1996).
10. K. van Dalen, S. Aravazhi, C. Grivas, S. García-Blanco, and M. Pollnau, "Thulium channel waveguide laser in a monoclinic double tungstate with 70% slope efficiency," *Opt. Lett.* **37**, 887-889 (2012).
11. E. Cantelar, J. A. Sanz-Garcia, G. Lifante, F. Cusso, and P. L. Pernas, "Single polarized Tm<sup>3+</sup> laser in Zn-diffused LiNbO<sub>3</sub> channel waveguides," *Appl. Phys. Lett.* **86**, 161119 (2005).
12. W. Bolaños, J. Carvajal, X. Mateos, E. Cantelar, G. Lifante, U. Griebner, V. Petrov, V. Panyutin, G. Murugan, J. Wilkinson, M. Aguiló, and F. Díaz, "Continuous-wave and Q-switched Tm-doped KY(WO<sub>4</sub>)<sub>2</sub> planar waveguide laser at 1.84  $\mu\text{m}$ ," *Opt. Express* **19**, 1449-1454 (2011).
13. D. Shepherd, D. Brinck, J. Wang, A. Tropper, D. Hanna, G. Kakarantzias, and P. Townsend, "1.9- $\mu\text{m}$  operation of a Tm:lead germanate glass waveguide laser," *Opt. Lett.* **19**, 954-956 (1994).
14. F. Fusari, R. Thomson, G. Jose, F. Bain, A. Lagatsky, N. Psaila, A. Kar, A. Jha, W. Sibbett, and C. Brown, "Lasing action at around 1.9  $\mu\text{m}$  from an ultrafast laser inscribed Tm-doped glass waveguide," *Opt. Lett.* **36**, 1566-1568 (2011).
15. D. Lancaster, S. Gross, H. Ebendorff-Heidepriem, K. Kuan, T. Monro, M. Ams, A. Fuerbach, and M. Withford, "Fifty percent internal slope efficiency femtosecond direct-written Tm<sup>3+</sup>:ZBLAN waveguide laser," *Opt. Lett.* **36**, 1587-1589 (2011).
16. R.V. Ramaswamy, R. Srivastava, "Ion-exchanged glass waveguides: a review," *J. Lightw. Technol.* **6**, 984-1000 (1988).
17. A. Choudhary, A.A. Lagatsky, K. Pradeesh, W. Sibbett, C.T.A. Brown, D.P. Shepherd, "Diode-pumped femtosecond solid-state waveguide laser with a 4.9 GHz pulse repetition rate," *Opt. Lett.* **37**, 4416-4418 (2012).
18. N. Leindecker, A. Marandi, R. Byer, K. Vodopyanov, J. Jiang, I. Hartl, M. Fermann, and P. Schunemann, "Octave-spanning ultrafast OPO with 2.6-6.1  $\mu\text{m}$  instantaneous bandwidth pumped by femtosecond Tm-fiber laser," *Opt. Express* **20**, 7046-7053 (2012).
19. T. Luo, S. Jiang, Y. Hu, G.N. Conti, S. Honkanen, S.B. Mendes, N. Peyghambarian, "Germanate glass channel waveguides for infrared waveguide lasers," *Quantum Electronics and Laser Science Conference, 1999. QELS '99.* **266** (1999).
20. D. L. Yang, E. Y.B. Pun, and H. Lin, "Tm<sup>3+</sup> doped ion-exchanged aluminum germanate glass waveguide for S-band amplification," *Appl. Phys. Lett.* **95**, 151106 (2009).
21. D. E. McCumber, "Einstein relations connecting broadband emission and absorption spectra," *Phys. Rev.* **136**, A954-A957 (1964).
22. L. Zhang, J. Zhang, C. Yu, and L. Hu, "A method for emission cross section determination of Tm<sup>3+</sup> at 2.0  $\mu\text{m}$  emission," *J. Appl. Phys.* **108**, 103117 (2010).
23. J.R. Salcedo, J.M. Sousa and V.V. Kuzmin, "Theoretical treatment of relaxation oscillations in quasi-three-level systems," *Appl. Phys. B*, **62**, 83-85 (1996).
24. W. Risk, "Modeling of longitudinally pumped solid-state lasers exhibiting reabsorption losses," *J. Opt. Soc. Am. B* **5**, 1412-1423 (1988).